JOURNAL OF APPLIED PHYSICS 115, 17B534 (2014)

Dopant spin states and magnetism of $Sn_{1-x}Fe_xO_2$ nanoparticles

A. Punnoose,[1,a)] Kelsey Dodge,[1] J. J. Beltrán,[1,2] K. M. Reddy,[1] Nevil Franco,[1] Jordan Chess,[1] Josh Eixenberger,[1] and C. A. Barrero[2]
[1]*Department of Physics, Boise State University, Boise, Idaho 83725-1570, USA*
[2]*Grupo de Estado Sólido, Facultad de Ciencias Exactas y Naturales, Universidad de Antioquia UdeA, Calle 70 No 52-21, Medellín, Colombia*

(Presented 6 November 2013; received 23 September 2013; accepted 28 January 2014; published online 28 March 2014)

This work reports detailed investigations of a series of ~2.6 nm sized, $Sn_{1-x}Fe_xO_2$ crystallites with x = 0–0.10 using Mossbauer spectroscopy, x-ray photoelectron spectroscopy (XPS), electron paramagnetic resonance spectroscopy (EPR), and magnetometry to determine the oxidation state of Fe dopants and their role in the observed magnetic properties. The magnetic moment per Fe ion μ was the largest $\sim 6.48 \times 10^{-3}$ μ_B for the sample with the lowest (0.001%) Fe doping, and it showed a rapid downward trend with increasing Fe doping. Majority of the Fe ions are in 3+ oxidation state occupying octahedral sites. Another significant fraction of Fe dopant ions is in 4+ oxidation state and a still smaller fraction might be existing as Fe^{2+} ions, both occupying distorted sites, presumably in the surface regions of the nanocrystals, near oxygen vacancies. These studies also suggest that the observed magnetism is not due to exchange coupling between Fe^{3+} spins. A more probable role for the multi-valent Fe ions may be to act as charge reservoirs, leading to charge transfer ferromagnetism.
 [http://dx.doi.org/10.1063/1.4869285]

Oxide semiconductors have been extensively researched as dilute magnetic semiconductors since Dietl *et al.*[1] predicted room temperature ferromagnetism (RTFM) in Mn-doped ZnO. RTFM has been reported in several oxide semiconductor systems doped with transition metal (TM) dopants[2] but also even in undoped oxides.[3,4] Observation of RTFM in several undoped oxide semiconductors, prepared in nanoscale form, led many to think that TM dopants have no role in the magnetism. However, it was shown that the magnetization of oxide nanoparticles increased systematically when doped with increasing concentrations of TM ions,[4,5] demonstrating that TM ions still play a role.[4–6] Interestingly, the ferromagnetic properties and their variation with TM dopant concentration are difficult to explain using any of the known exchange mechanisms. Thus, it is important to determine the exact oxidation and spin states of TM dopants to understand their actual role in producing magnetism. To investigate this, a series of ~2.6 nm sized single-phase $Sn_{1-x}Fe_xO_2$ crystallites were synthesized by reacting tin (IV) acetate ($Sn(C_2H_4OH)_4$), urea ($C_2O_2(NH_3)_2$), and appropriate amounts of iron (II) acetate ($Fe(C_2H_4OH)_2$) as discussed in detail elsewhere.[4] The samples were characterized and phase purity confirmed using procedures described elsewhere.[7–9]

In a recent study,[10] we have investigated the magnetic properties of similar $Sn_{1-x}Fe_xO_2$ nanocrystals, with x in the 0.1% to 20% range and found that the sample magnetization increases with increasing Fe%. Even the undoped pure SnO_2 nanoparticles showed a weak ferromagnetic behavior characterized by a saturation magnetization $M_s = 0.31 \pm 0.01$ memu/g and coercivity $H_c = 91$ G. Interestingly, introduction of just 0.1% Fe dopants into these SnO_2 nanocrystals almost doubled the M_s to 0.671 memu/g. M_s showed a gradual and systematic increase with increasing Fe concentration, reaching a maximum (1.52 memu/g) at 2.5% Fe (see Fig. 1(a), inset), confirming that the dopant Fe ions indeed play an important role in the magnetic properties. The magnetic moment per Fe ion μ showed a downward trend with increasing Fe%, as shown in Fig. 1(a). μ was the largest $\sim 1.6 \times 10^{-4}$ μ_B for the sample with the lowest (0.1%) Fe doping. This prompted us to make three new samples with much lower Fe% of 0.01%, 0.005%, and 0.001% to see if this trend continues for still lower Fe concentrations. Interestingly, these samples with extremely small dopant concentrations indeed followed the same trend and μ showed orders of magnitude increase, reaching 64.8×10^{-4} μ_E for 0.001% Fe doping. Although the M_s is relatively weak in all these samples, these results were clearly reproducible in three independently synthesized batches.[4] Although, the M_s value increased systematically with increasing x, especially in the 0% to 2.5% Fe range μ, calculated by assuming that all the dopant Fe ions contribute to the observed M_s is unusually low, and it decreased rapidly with increasing x, almost following a 1/x dependence (see Fig. 1(a)). Even the maximum μ of 64.8×10^{-4} μ_B observed for the 0.001% Fe doped sample is way smaller than the expected spin-only contribution from either high or low spin Fe^{3+} ions. Appearance of RTFM in undoped SnO_2 nanoparticles and the extremely low moment observed in Fe doped samples makes it difficult to explain the ferromagnetism in $Sn_{1-x}Fe_xO_2$ nanoparticles using any of the conventional magnetic exchange interactions between the dopant spins. The observed RTFM was not due to any impurity inclusions since similar RTFM was observed in multiple samples[4] of separately synthesized pure SnO_2 that were thoroughly analyzed for any evidence of impurities. It is also observed that M_s increased linearly with the amount of analyzed mass for pure SnO_2 as shown in Fig. 1(b).

a)Author to whom correspondence should be addressed. Electronic mail: apunnoos@boisestate.edu.

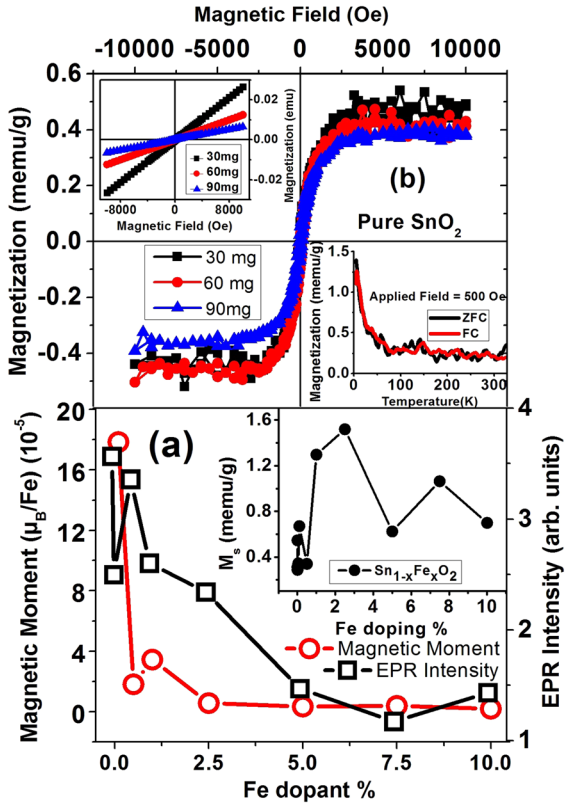

FIG. 1. (a) Magnetic moment per Fe ions and the Fe^{3+} EPR signal intensity of $Sn_{1-x}Fe_xO_2$, both plotted as a function of Fe dopant % at 300 K; inset in panel (a) shows the variation of M_s as a function of Fe dopant %. (b) Hysteresis loops of three undoped SnO_2 samples with increasing sample mass (30, 60, and 90 mg), showing linear relation between saturation magnetization and weight. These plots were obtained from the raw data shown in the inset (top left), after correcting for the background signal from the sample holder and subtracting the linear paramagnetic component. The lower right inset in Fig. 1(b) presents the FC and ZFC magnetization of a 5% Fe doped SnO_2 sample, plotted as a function of temperature.

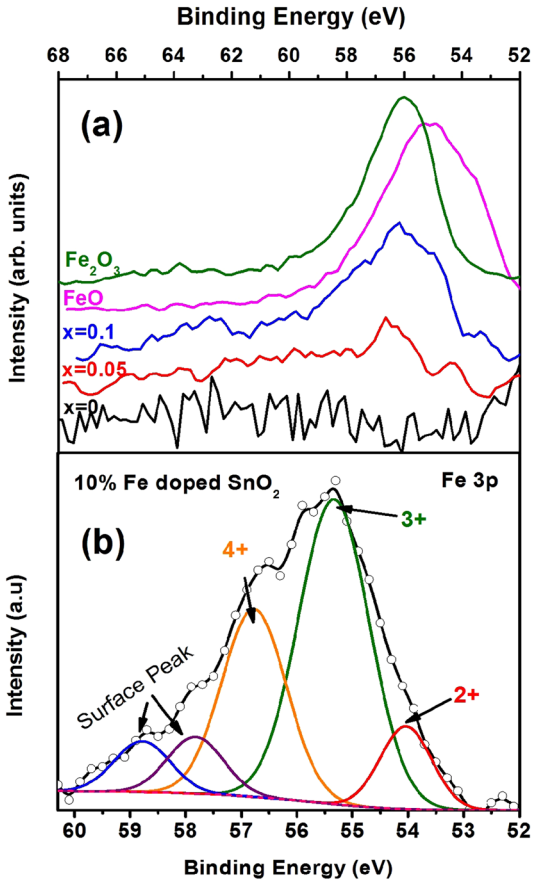

FIG. 2. (a) Fe 3p region of the XPS spectra of different samples indicated. (b) Core level spectra of Fe 3p region deconvoluted to indicate the presence of different oxidation states of Fe. Circles are experimental data points and the black curve is the simulated spectrum.

Magnetization from impurity phases would not result in such a linear scaling with the amount of sample. Magnetization of the 5% Fe doped SnO_2 was measured in the 5 to 325 K range using a constant applied field of 500 Oe, both in the zero field cooled (ZFC) and field cooled (FC) modes (lower right inset of Figure 1(b)). The FC and ZFC curves did not show any divergence, thus ruling out the presence of any blocked or superparamagnetic phases. Instead, the M vs T curves followed a Curie law behavior, expected from the predominant paramagnetic component that is also observed in the linear M vs H data (top left inset of Figure 1(b)).

To determine the oxidation and spin state of the doped Fe ions and their role in the observed weak ferromagnetism, detailed XPS, electron paramagnetic resonance (EPR), and Mossbauer spectroscopy studies of Fe-doped SnO_2 nanocrystals were carried out. In XPS analysis, the Fe 3p signal was used instead of Fe 2p which is overlapped by strong Sn 3p peaks. The Fe 3p signal intensity increased with increasing Fe% (Fig. 2(a)). All the $Sn_{1-x}Fe_xO_2$ samples had a Fe 3p peak near 56.1 eV, which is higher than the reported values of metallic Fe (53 eV) and common Fe oxides including Fe_3O_4 (53.9 eV), FeO (54.9 eV shown), and Fe_2O_3 (55.4 eV shown).[11] This indicates that Fe is not present as any of the common iron oxides and its chemical environment is different from that in these oxides. Fig. 2(b) presents the deconvoluted spectrum of the Fe 3p core level area of the 10% Fe doped SnO_2 sample which indicates the presence of Fe^{2+}, Fe^{3+}, and Fe^{4+} states[12,13] in this sample. The main peak at 55.63 eV binding energy is attributed to the Fe^{3+} state and a weaker peak at a lower binding energy 54.04 eV is assigned to Fe^{2+} ions. Also, a peak with moderate intensity at the higher binding energy of 56.5 eV is allocated to Fe^{4+} oxidation state. Thus, these XPS data indicate the presence of multivalent Fe ions in the sample. Two weaker peaks with larger FWHM, appearing at still higher binding energies, are assigned to surface peaks owing to the extensive surface contributions from these ~2.6 nm sized nanoparticles.[12]

Fig. 3 shows the ^{57}Fe Mössbauer spectra of $Sn_{1-x}Fe_xO_2$ ($x = 0.05$ and 0.10) samples at RT, and the derived hyperfine parameters are shown in Table I. These Mössbauer spectra consisted of only doublets indicative of paramagnetic or superparamagnetic states, but no sixtets indicative of a magnetically coupled component was evidenced within the detection limit of the technique. In both samples, the spectra exhibited a considerable asymmetry. The paramagnetic signals in these samples were properly fitted with two doublets, D1 and D2, respectively, indicating two different oxidation states. Hyperfine parameters of D1 for both samples, 5% and 10% Fe doped SnO_2, suggest that these Fe ions are in high spin 3+ state, in an octahedral environment, while isomeric

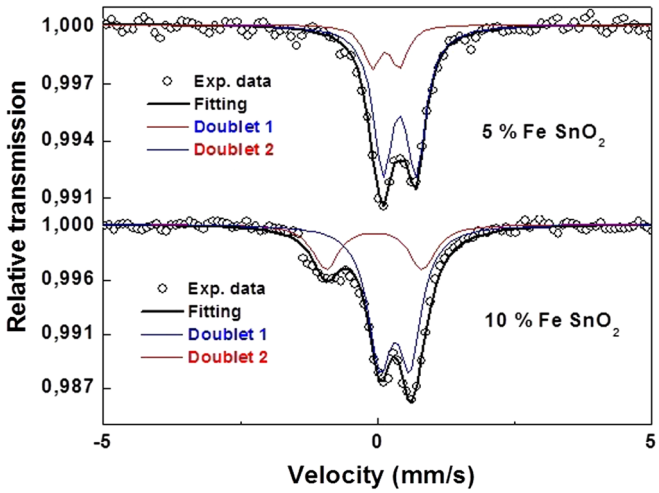

FIG. 3. RT ^{57}Fe Mössbauer spectra for $Sn_{1-x}Fe_xO_2$ with x = 0.05 (top panel) and 0.10 (bottom panel).

shift of D2 (−0.06–0.14) lies in the range for Fe^{4+} ions. 10% Fe doped SnO_2 sample shows higher quadrupole splitting than 5%Fe doped SnO_2 sample, probably indicating that the Fe^{4+} ions occupy highly distorted sites close to oxygen vacancies. From these hyperfine parameters obtained, it can be seen that the quadrupole splitting of D2 changes drastically when Fe doping is increased, indicating changes in chemical environment of these Fe^{4+} ions with increasing Fe %. The observation that the relative areas of D1 for those samples are always higher than D2 indicate that Fe^{3+} ions are in higher proportion than Fe^{4+} ions. The fact that D1 corresponds to Fe^{3+} ions occupying octahedral sites and that it constitutes 79% (in 5% Fe doped SnO_2) and 71% (in 10% Fe doped SnO_2) of the total area makes us to assign them to Fe^{3+} dopant ions incorporated primarily in the octahedral Sn^{4+} sites in the core of the nanocrystals. The second doublet due to Fe^{4+} in distorted sites and occupying 21%–29% area is most likely due to Fe ions occupying surface sites. In a nanocrystal of size ∼2.6 nm, it is likely that ∼21%–29% of Sn sites are on the surface. Surface of nanoparticles usually have plenty of defects including oxygen vacancies (V_o) and increased doping can enhance the oxygen vacancy concentration, justifying the higher quadrupole splitting observed in the 10% Fe doped SnO_2 samples. Presence of V_o on the nanoparticle surface facilitates distorted sites suitable for Fe^{4+}, and with increasing Fe doping, more V_o and Fe^{4+} are created on the nanoparticle surface.

EPR spectra of the samples also confirmed the presence of high spin Fe^{3+} ions in octahedral sites,[14] and their intensity (area under the absorption curve) decreased systematically with x, as shown in Fig. 1(a). This may be partially due to the conversion of increasing fractions of the Fe^{3+} ions to Fe^{4+}/Fe^{2+}states, and this might also contribute to the decrease in magnetic moment μ with x (Fig. 1(a)). Interestingly, a broad ferromagnetic resonance (FMR) signal expected from magnetic systems formed by exchange coupling between the high spin Fe^{3+} ions is missing in these samples. Absence of a sixtet spectrum in the Mossbauer spectra along with this result rules out the presence of ferromagnetic or antiferromagnetic interactions between the high spin Fe^{3+} ions. Presence of multivalent Fe ions (2+, 3+, and 4+ states) and absence of conventional magnetic exchange interaction between the spins suggest that the observed magnetism may be due to unconventional mechanisms such as charge transfer ferromagnetism[1] involving multivalent Fe ions and oxygen defects.

TABLE I. RT ^{57}Fe Mössbauer parameters of $Sn_{1-x}Fe_xO_2$ ($x = 0.05$ and 0.10) samples. Estimated errors are of about ± 0.01 mm/s for the isomer shift δ, the quadrupole splitting Δ, and the linewidth Γ, and of about ±2% for the relative area, A. D1 and D2 are doublet 1 and doublet 2, respectively.

Sample	Component	δ (mm/s)	Δ (mm/s)	Γ (mm/s)	A (%)
5% Fe doped SnO_2	D1	0.39	0.60	0.21	79
	D2	0.14	0.50	0.19	21
10% Fe doped SnO_2	D1	0.32	0.55	0.23	71
	D2	−0.06	1.75	0.30	29

It has been shown both theoretically and experimentally that low levels of Fe doping in oxide semiconductor nanoparticles can strongly reduce the energy for oxygen vacancy formation.[15] For low doping levels, the well separated Fe^{3+} ions can act as efficient e^- as well as h^+ traps, turning into Fe^{2+} or Fe^{4+} states, respectively.[16] Thus, the observation of Fe^{4+} and even Fe^{2+} states in our samples is not unexpected, although Fe^{4+} ions have only rarely been reported in the past. Presence of 2+, 3+, and 4+ oxidation states and oxygen vacancies/defects in these 2.6 nm $Sn_{1-x}Fe_xO_2$ forms a potential recipe for RTFM according to the charge transfer ferromagnetism model.[17]

This work was supported by the National Science Foundation Grants DMR-1137419 and CBET 1134468.

[1]T. Dietl *et al.*, Science **287**, 1019–1022 (2000).
[2]J. M. D. Coey *et al.*, Nature Mater. **4**(2), 173–179 (2005).
[3]A. Sundaresan *et al.*, Phys. Rev. B **74**, 161306 (2006).
[4]G. A. Alanko *et al.*, J. Appl. Phys. **111**, 07C321 (2012).
[5]L. M. Johnson *et al.*, Phys. Rev. B **82**(5), 054419 (2010).
[6]J. M. D. Coey *et al.*, New J. Phys. **12**, 053025 (2010).
[7]J. Anghel *et al.*, J. Appl. Phys. **107**, 09E314 (2010).
[8]A. Punnoose *et al.*, Nanotechnology **18**, 165502 (2007).
[9]A. Punnoose *et al.*, J. Appl. Phys. **109**, 07C305 (2011).
[10]K. Dodge *et al.*, J. Appl. Phys. **113**, 17B504 (2013).
[11]D. Brion, Appl. Surf. Sci. **5**(2), 133–152 (1980).
[12]A. P. Grosvenor *et al.*, Surf. Interface Anal. **36**, 1564 (2004).
[13]M. Descostes *et al.*, Appl. Surf. Sci. **165**(4), 288–302 (2000).
[14]A. Punnoose *et al.*, Appl. Magn. Reson. **36**, 331–345 (2009).
[15]A. Roldan *et al.*, J. Phys. Chem. C **114**, 6511 (2010).
[16]M. Asiltürk *et al.*, J. Photochem. Photobiol. A: Chem. **203**, 64 (2009).
[17]J. M. D. Coey *et al.*, J. Phys. D: Appl. Phys. **41**(13), 134012 (2008).